Microelectronics and Reliability Pergamon Press 1970. Vol. 9, pp. 177–186. Printed in Great Britain

STATE-VARIABLE AND GYRATOR REALIZATIONS FOR COMPLETE INTEGRATION: A COMPARISON

M. B. WALDRON and R. W. NEWCOMB

Stanford Electronics Laboratories, Stanford, California 94305

Abstract—For complete integration of a given transfer function, the number, size and spread of components will be of prime interest, in contrast, for example, to sensitivity. To illustrate these properties, a given degree three Cauer response is synthesized in five ways with emphasis upon complete integration. The results, based primarily upon gyrator and state-variable techniques, are readily compared.

"When a man speaks words of truth he speaks words of greatness: know the nature of truth."(1)

1. INTRODUCTION

ALTHOUGH complete integration of linear transfer functions still appears to be several years away, it seems bound to occur. As a consequence there is some value in evaluating the changes necessary over present technology as well as the various alternative ways of proceeding. This paper is a contribution to the latter and proceeds by synthesizing five likely candidates for the complete integration of a specific response characteristic.

In order to be somewhat clear in our terminology we consider a completely integrated circuit to be one in which all components are processed simultaneously on a single chip. This is to be taken in contrast to lumped circuits, or partially integrated ones, where, respectively, either all components (e.g. resistors, transistors, capacitors) or only some (e.g. operational amplifiers, resistors, capacitors) are separately manufactured and later brought together in a circuit construction.

Because of their inherent importance to integrated circuit technology, effort is concentrated here upon state-variable and gyrator type active RC circuits. But, in contrast to their lumped or partially integrated counterparts, attention is paid to the total capacitance and resistance as well as their spread. The purpose for this is, of course, that larger total capacitance and resistance generally means larger chip size, while fabrication ease generally favours identical components. Too, there is some interest in the circuit layout, for the avoidance of crossing leads, for example. In contrast to the lumped case, size of the active components is not such a critical factor because most integrated active elements are relatively compact and, thus, the number of operational amplifiers or gyrators is not so important for size purposes, though this number should be kept small for power dissipation purposes. Finally, we mention that for integration there are reasonable ranges over which component values can vary, due to processing procedures and material properties.

With these points in mind we have developed the following circuits whose component values in our view have been chosen somewhat optimum for the design method considered when used with monolithic integrated circuit technology. The transfer function chosen is a realistic one for the techniques envisaged, and one which is more than degree two but of sufficient simplicity to illustrate the major points without undue complexity. We take as general background the material through Section 7 of (2), this paper being possibly considered an addition to that section.

"When a man knows, he can speak truth. He who does not know cannot speak truth: know the nature of knowledge."(1)

2. DESIGN SPECIFICATIONS

The specifications to be realized are as shown in Fig. 1a. That is, a voltage transfer device is specified with a passband of 0–7 kHz with no more than 1 dB of attentuation allowed in the passband. Above 10 kHz an attenuation of at least 20 dB is required. Where necessary we shall take load and source resistance to be 600 Ω.

From these specifications a transfer function is rather readily obtained. For this purpose we use the convenient design tables of Skwirzynski (Ref. (3), pp. 289–375) from which we find that a degree three structure will satisfy the requirements (Ref. (3), pp. 37, 290) (for $k = 0{\cdot}7$, $D_p = 1$ dB; $D_a = 23$ dB). This determines the normalized Cauer response of Fig. 1b where the terminology, as at other relevant places below, follows that of Skwirzynski. From the mentioned tables it follows readily that the normalized transfer function of interest is:

$$\frac{V_2}{V_s}(p) = H\frac{0{\cdot}56617p^2+1}{p^3+0{\cdot}80867p^2+0{\cdot}87177p+0{\cdot}36495} \tag{1a}$$

$$= H\frac{1}{p+0{\cdot}50766}\times\frac{0{\cdot}56617p^2+1}{p^2+0{\cdot}301014p+0{\cdot}71898} \tag{1b}$$

Again from the $n = 3$ tables of Skwirzynski the normalized inductor tee and capacitor pi circuits of Fig. 2 are determined to yield equation (1). As is standard practice, to denormalize we determine an impedance scaling constant $r_n = 600$ and a frequency scaling $\omega_B = 5{\cdot}26\times10^4$ (as ascertained from Fig. 1b). With these, all resistances are raised by $r_n = 600$, all capacitances by $1/(r_n\omega_B) = 3{\cdot}16\times10^{-8}$, and all inductances by $r_n/\omega_B = 1{\cdot}14\times10^{-4}$. As can be seen from the table of parameter values included in Fig. 2, this denormalization yields capacitors of nanofarad (10^{-9}f) size, which, however, are too large for reasonable integration. Also, something must be done about the inductors.

"When a man thinks then he can know. He who does not think does not know: know the nature of thought."(1)

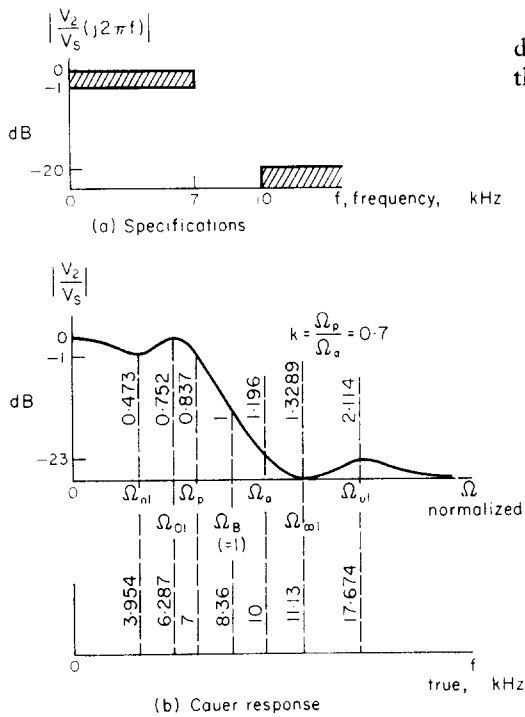

Symbol	Normalized	True f, kHz
Ω_{nl}	0·473	3·954
Ω_{ol}	0·752	6·287
Ω_p	0·837	7
$\Omega_B=\sqrt{(\Omega_p\Omega_a)}$	1	8·36
Ω_a	1·196	10
$\Omega_{\omega l}=1/\Omega_{ol}$	1·3289	11·13
$\Omega_{vl}=1/\Omega_{nl}$	2·114	17·674

FIG. 1. Response specifications. (a) Specifications; (b) Cauer response.

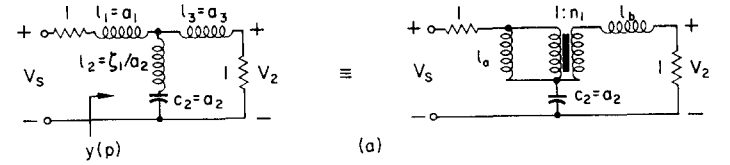

(a)

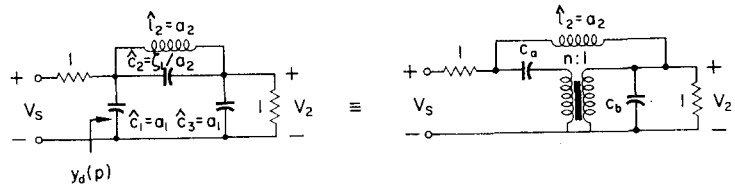

(b)

Parameter	Normalized	True
$r_s = r_l$	1	600Ω
$l_1 = l_3 = \hat{c}_1 = \hat{c}_3 = a_1$	1·9698	22·6mH,62·3nF
$\hat{l}_2 = c_2 = a_2$	0·8373	9·54mH,26·4nF
ζ_1	0·56617	
$l_2 = \hat{c}_2 = \zeta_1 / a_2$	0·676	7·70mH,21·4nF
$l_a = c_a = a_1 + (\zeta_1/a_2)$	2·646	30·2mH,83·7nF
$l_b = c_b = \frac{a_1(a_1+2\zeta_1/a_2)}{a_1+\zeta_1/a_2}$	2·495	27·4mH,78·8nF
$n_1 = \zeta_1/(a_1a_2+\zeta_1)$	0·291	0·291
H	2·7397	2·7397

(c)

FIG. 2. Designs from tables. (a) Inductive Tee structure; (b) capacitive Pi structure; (c) parameter values.

3. TEE STRUCTURE DENORMALIZATION

By the insertion of a gyrator after the input source resistance, and another one at the output to cancel it, the inductor tee of Fig. 2a is turned into its dual, this dual being the capacitor pi of Fig. 2b. The gyrator parameter gives an added degree of freedom which can be used to bring the nanofarad capacitances down to picofarads, as illustrated in Fig. 3. In Fig. 3 the central portion uses the floating inductor replacement attributed to Holt and Taylor[4] to replace the central inductor of Fig. 2b by a grounded gyrator–capacitor–gyrator cascade; again another degree of freedom through the gyrator conductance g_1 is introduced. Reasonable choices for all element values are given in the table of Fig. 3b where it is noticed that, although the capacitor spread is relatively small, there is a relatively large spread in gyration conductances. It should be observed too that an extra capacitor, over the minimum number of three

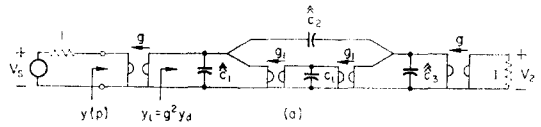

Parameter	Normalized	True
$r_s = r_l$	1	600Ω
1/g	free	31·6Ω
$\hat{\hat{c}}_1 = \hat{\hat{c}}_3$	$g^2\hat{\hat{c}}_1$	62·3pF
$\hat{\hat{c}}_2$	$g^2\hat{\hat{c}}_2$	21·4pF
$1/g_1$	free	316kΩ
c_1	$g_1^2\hat{\hat{l}}_2/g^2$	95·4pF

(b)

FIG. 3. Table replacement design. (a) Normalized gyrator replacements; (b) parameter values.

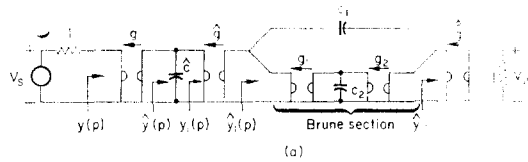

Parameter	Normalized	True
$r_s = r_l$	1	600Ω
1/g	Free	12kΩ
$\hat{c}$	$2{\cdot}473g^2$	195pF
$1/\hat{g}$	free = 10/g	120kΩ
c_1	$3{\cdot}017(\hat{g}/g)^2$	302pF
c_2	free	32pF
$1/g_1$	$0{\cdot}991(g/\hat{g})/\omega c_2$	19kΩ
$1/g_2$	$0{\cdot}250(g/\hat{g})/\omega c_2$	4·7kΩ
$1/\hat{g}$	$0{\cdot}2556g/\hat{g}$	1·5kΩ

(b)

FIG. 4. Gyrator cascade design. (a) Cascade structure; (b) parameter values.

required for the transfer function of equation (1), is used. Thus excess processing will most likely be necessary in implementing the design of Fig. 3.

"When a man has faith then he thinks. He who has not faith does not think: know the nature of faith."[1]

4. GYRATOR–CASCADE SYNTHESIS

A result of the same structural form as the circuit of Fig. 3 but using the minimum number of capacitors is obtained by a direct cascade synthesis in non-reciprocal form.[5] The result, given in Fig. 4, follows by using, step by step, the sequence of calculations outlined in Ref. (2), pp. 165–167. This begins by obtaining a suitable input admittance to synthesize. For this we can use the admittance $y(p)$ of the inductor tee circuit given in Fig. 2a. In terms of the parameters and values given by Skwirzynski, and appearing in Fig. 2, we find:

In terms of Fig. 4 the process consists of (1) removing the gyrator g for capacitance scaling (giving $\hat{y}(p) = g^2/y(p)$), (2) removing the shunt capacitor $\hat{c}$ for a zero of transmission at infinity (giving a remainder admittance $y_1(p) = \hat{y}(p) - 2{\cdot}47319g^2p = g^2\dfrac{0{\cdot}14467p^2 + 1{\cdot}46641p + 1}{2{\cdot}21547p^2 + 0{\cdot}8373p + 1}$), (3) removing another gyrator $\hat{g}$ for further capacitance scaling (giving $\hat{y}_1(p) = \hat{g}^2/y_1(p)$), (4) removing a non-reciprocal Brune section for a zero of transmission at $j\Omega_{\infty 1} = j\,1{\cdot}3289$ ($\hat{y}_1(p)$ has a zero of its even part at $p = j\Omega_{\infty 1}$; Richards' theorem is then applied using $k = j\Omega_{\infty 1}$ and then $k_1 = -j\Omega_{\infty 1}$ to extract the Brune section; $\hat{y}_{11}(p) = \hat{g}^2/0{\cdot}0653g^2$), (5) the final gyrator $\hat{g}$ removal to yield a unit load resistance for equal source and load terminations.

Judicious choice of the free parameters is next made to obtain element values which are reasonable for a complete integration, upon a denormalization. These free parameters are equivalent to the three gyration conductances, but are taken as g, $\hat{g}$

$$y(p) = \frac{a_2(a_1+[\zeta_1/a_2])p^2+a_2p+1}{a_1a_2(a_1+2[\zeta_1/a_2])p^3+a_2(a_1+[\zeta_1/a_2])p^2+2a_1p+1} \tag{2a}$$

$$= \frac{2{\cdot}2154p^2+0{\cdot}8373p+1}{5{\cdot}4786p^3+2{\cdot}2154p^2+3{\cdot}9396p+1} \tag{2b}$$

c_2 for convenience. The final results are shown in Fig. 4 where, as with Fig. 3, it should be observed that all gyrators are conveniently grounded. It should also be observed that, although only three capacitors are used, a very high degree of accuracy is needed in making the numerical calculations. Apparently for this reason, a similar accuracy is needed in maintaining the gyrator conductance ratios for the Brune section gyrators in practical operation of the circuit.[6] Although the element value spread is reasonable too, it is higher than ideally desired.

"Where there is progress one sees and has faith. Where there is no progress there is no faith: know the nature of progress."[1]

5. OPERATIONAL AMPLIFIER STATE-VARIABLE SYNTHESIS

In order to cut down on the element value spread we next synthesize following the state-variable cascade synthesis.[7] For this synthesis to be in the desired cascade form we use the factored form of equation (1b); of course, cascade configurations are convenient for integrated layouts since crossing and feedback leads are most easily avoided. To proceed, equation (1b) is further decomposed to exhibit the constant at infinity in the degree two factor:

$$\frac{V_2}{V_s}(p) = H\frac{1}{p+0{\cdot}50766} \times \left[0{\cdot}56617 + \frac{-0{\cdot}1703p+0{\cdot}59214}{p^2+0{\cdot}301014p+0{\cdot}71898}\right] \tag{3}$$

Using the (unnormalized) negative gain integrator of Fig. 5a, where very reasonable element values occur for integration, the (normalized) block diagram type structure of Fig. 5b results directly from the state-variable equations. For the degree two portion (left-hand part of Fig. 5b) these equations are read directly from the transformed transfer function decomposition of equation (3) to be (Ref. (2), pp. 69, 75):

$$\frac{p}{\lambda}\begin{bmatrix}X_1\\X_2\end{bmatrix} = \begin{bmatrix}0 & 1\\ \dfrac{-0{\cdot}71898}{\lambda} & \dfrac{-0{\cdot}30104}{\lambda}\end{bmatrix}\begin{bmatrix}X_1\\X_2\end{bmatrix} + \begin{bmatrix}0\\ \dfrac{1}{\lambda}\end{bmatrix}V_s \tag{4a}$$

$$V_0 = [0{\cdot}59214, -0{\cdot}1703]\begin{bmatrix}X_1\\X_2\end{bmatrix} + 0{\cdot}56617\,V_s \tag{4b}$$

where $-\lambda = 76{\cdot}1 = 1/RC\omega_B$ is determined by the integrator constant fixed by the element values chosen in Fig. 5a. By appropriately and properly dimensioning the adders (Ref. (2), p. 71), Fig. 6 results when the same technique is also applied to the degree one portion.

In Fig. 6, although a slightly large resistance spread occurs, all component sizes are appropriate for integration; it should be observed that the integrators are identical and that the minimum number of reasonable sized capacitors is contained. However, the circuit does contain a large number of components, including seven operational amplifiers, in which case power dissipation and chip heating are points of concern.

"Where there is creation there is progress. Where there is no creation there is no progress: know the nature of creation."[1]

6. LOW-GAIN, LUMPED-DISTRIBUTED DESIGN

The number of amplifiers can be reduced to one while retaining reasonable element values by using the low-gain structures developed by Kerwin.[8] Of most interest is the lumped-distributed structure of Fig. 7a. To obtain the element values appropriate to Fig. 7a one needs to further frequency scale to bring the numerator zeros of equation (1a) to $\pm j1$. Thus, set $p^2_n = 0{\cdot}56617p^2$, or $p = 1{\cdot}32889p_n$; the degree two factor in equation (1b) becomes

$$T_2(p_n) = H_2\frac{p^2_n+1}{p^2_n + 0{\cdot}223488p_n + 0{\cdot}407065} \tag{5}$$

which has poles at $p_{n1,\,2} = -0{\cdot}112744 \pm j0{\cdot}62815$. The use of the appropriate design chart (Ref. (2), p. 91), entered at these poles, fixes the gain, $K = 1{\cdot}04$, and the normalized amplifier input

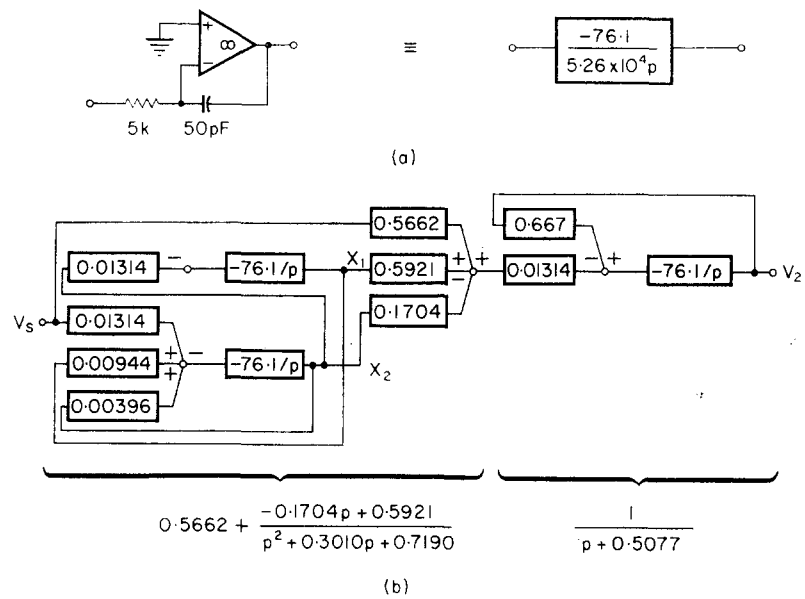

FIG. 5. State-variable realization. (a) Negative-gain integrator; (b) block structure.

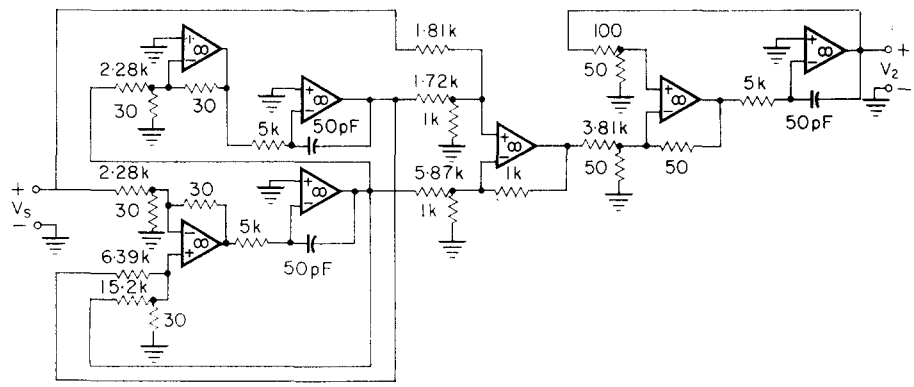

FIG. 6. State-variable circuit.

capacitance, $C = 0{\cdot}046$; the feedback resistor was previously normalized to $R_0 = 1$ while the distributed line values of $r = 17{\cdot}786$ and $c = 0{\cdot}629$ are fixed, on knowing R_0, by the requirement of a zero at $p_n = \pm j1$. Choosing $r_n = 10^4$ and $\omega'_B = (1{\cdot}329)(5{\cdot}26 \times 10^4) = 6{\cdot}99 \times 10^4$ fixes the denormalization of the degree two portion. For the degree one factor in equation (1b) an RC voltage divider is used for which a 40 kilohm resistance level is chosen to bring the capacitor value down to within reason; this capacitor is frequency denormalized through the previous ω_B. Note that this method has the advantage of letting the different sections use different denormalizations giving extra freedom in obtaining reasonable element values.

Although Fig. 7a shows a relatively large spread in element values, especially when compared with Fig. 6, the overall circuit is quite compact due to the small number of components. In order to see this size advantage of distributed circuits an analogous lumped structure was designed (Ref. (2), p. 89), as shown in Fig. 7b. From this

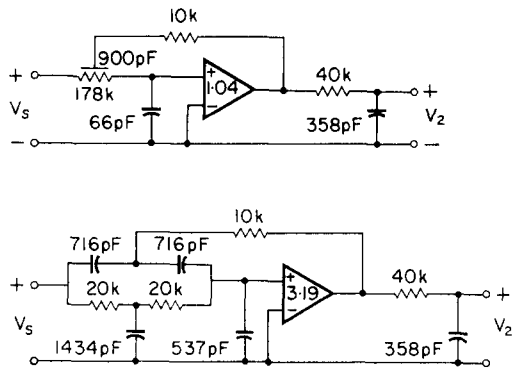

FIG. 7. Low-gain realizations. (a) Lumped-distributed; (b) lumped equivalent.

latter we see that the use of a distributed line has allowed almost a three-to-one saving in capacitor area. It has reduced, too, the gain from about three to very near unity, allowing simpler amplifier designs and possibly higher frequency ranges of operation.

"Where there is joy there is creation. Where there is no joy there is no creation: know the nature of joy."[1]

7. STATE-SPACE GYRATOR SYNTHESIS

Having considered the previous methods it is instructive to investigate a recent technique which combines the state-space and gyrator philosophies.[9] The method involves the gyrators in a passive synthesis of an admittance matrix derived from the state-variable equations. The latter equations are first transformed to guarantee the passivity of the resultant admittance matrix with the state-variable equations resulting upon a termination of the gyrator circuit, which also contains a resistor, in unit capacitors (the capacitor voltages are the state variables with these capacitor currents giving the derivatives in the state-variable equations). In contrast to the operational amplifier state variable synthesis where factorization to give degree two (or one) equations are used for coefficient sensitivity reasons, the present method gives a direct state-variable realization of the total transfer function.

We proceed by using literal coefficients, rewriting equation (1a), with $H = 1$ chosen for convenience, as

$$\frac{V_2}{V_s}(p) = \frac{c_2 p^2 + 1}{p^3 + \alpha_3 p^2 + \alpha_2 p + \alpha_1} \tag{6}$$

From equation (6) we are directly led to the time-domain state-space equations

$$\frac{dx_0(t)}{dt} = A_0 x_0(t) + B_0 v_s(t), \quad v_2(t) = C_0 x_0(t) \tag{7a}$$

with

$$A_0 = \begin{bmatrix} 0 & 1 & 0 \\ 0 & 0 & 1 \\ -\alpha_1 & -\alpha_2 & -\alpha_3 \end{bmatrix}, \quad B_0 = \begin{bmatrix} 0 \\ 0 \\ 1 \end{bmatrix}, \quad C_0 = (1,0,c_2) \tag{7b}$$

and $x_0(t)$ the state 3-vector. In order to guarantee passivity of the result we make a change of the state through the transformation $x_0 = Px$ with P resulting from factoring $K = P\tilde{P}$, $\sim$ denoting the matrix transpose; a positive definite K in turn is obtained by solving the matrix equation

$$A_0 K + K\tilde{A}_0 = -[0_2 \dot{+} 1]. \tag{8a}$$

Here $\dot{+}$ denotes the direct sum and 0_2 is the 2×2 zero matrix. The passive coupling network 5×5 admittance matrix of interest is given by

$$Y_c = \begin{bmatrix} 0 & 0 & \tilde{B}_0 \tilde{P}^{-1} \\ 0 & 0 & C_0 P \\ -P^{-1}B_0 & -\tilde{P}\tilde{C}_0 & -P^{-1}A_0 P \end{bmatrix} \tag{8b}$$

One can check, by inserting voltage and current variables, that loading the final three ports of the five-port described by Y_c in unit capacitors results in equations (7), and hence (6) (after a unit gyrator is inserted at port two to convert this admittance current to the output transfer function voltage).

We find on solving equation (8a), using (7b) and factoring K into $P\tilde{P}$,

$$K = [k_{ij}] = \frac{1}{2(\alpha_2\alpha_3 - 1)} \begin{bmatrix} \alpha_3/\alpha_1 & 0 & -1 \\ 0 & 1 & 0 \\ -1 & 0 & \alpha_2 \end{bmatrix}, \tag{9a}$$

$$P = \begin{bmatrix} \sqrt{k_{11}} & 0 & 0 \\ 0 & \sqrt{k_{22}} & 0 \\ \dfrac{-k_{22}}{\sqrt{k_{11}}} & 0 & \sqrt{\left(\dfrac{k_{11}k_{33} - k^2_{22}}{k_{11}}\right)} \end{bmatrix}$$

which for the numbers on hand ($\alpha_1 = 0{\cdot}36495$, $\alpha_2 = 0{\cdot}87177$, $\alpha_3 = 0{\cdot}80867$, $c_2 = 0{\cdot}56617$) gives

$$P = \begin{bmatrix} 1{\cdot}806 & 0 & 0 \\ 0 & 1{\cdot}213 & 0 \\ -0{\cdot}814 & 0 & 0{\cdot}781 \end{bmatrix}, P^{-1} = \begin{bmatrix} 0{\cdot}5535 & 0 & 0 \\ 0 & 0{\cdot}825 & 0 \\ 0{\cdot}5755 & 0 & 1{\cdot}281 \end{bmatrix} \quad (9b)$$

or, finally, for equation (8b)

$$Y_c = \left[\begin{array}{cc|ccc} 0 & 0 & 0 & 0 & 1{\cdot}281 \\ 0 & 0 & 1{\cdot}346 & 0 & 0{\cdot}442 \\ \hline 0 & -1{\cdot}346 & 0 & -0{\cdot}672 & 0 \\ 0 & 0 & 0{\cdot}672 & 0 & -0{\cdot}644 \\ -1{\cdot}281 & -0{\cdot}442 & 0 & 0{\cdot}644 & 0{\cdot}809 \end{array}\right] \quad (10)$$

This admittance is synthesized by five gyrators and one (positive) resistor to give the structure shown shown in Fig. 8. On loading the circuit for Y_c in unit capacitors the normalized transfer function of equation (1) results when also a unit gyrator is cascaded at the output port (port number two).

Since a voltage transfer function is on hand, we can arbitrarily impedance scale to get desired element values. On scaling to as reasonable numbers as seem possible, having $C = 250$ pF and hence $r_n = 76$ kΩ (since ω_B is fixed), we obtain the final circuit of Fig. 8. In Fig. 8 we note that all components are grounded, an advantage for complete integration, since, for example, all capacitors can use a common substrate for one plate. The single resistor can be transformed through the input gyrator to yield a series source resistance of 37·5 kΩ. We see then that large, but possible, element values result for integration while the layout, as with all of the previous, can be made with no lead crossings outside of those necessary for bias circuits.

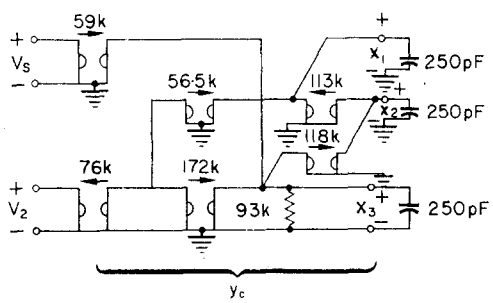

FIG. 8. State-variable gyrator realization, $H = 1$.

"Where there is the Infinite there is joy. There is no joy in the finite: know the nature of the Infinite."[1]

8. CONCLUSIONS

By considering the design of an actual response which may be desired, several design methods can be compared for their suitability toward integration. To facilitate this comparison we have given five different designs for the Cauer degree three response specified in Fig. 1. Having already considered the circuits separately, it is appropriate at this point to compare them with regard to the factors of most interest for complete integration. This is done in Table 1 where total element values and spreads are given (as obtained from the previous figures). From Table 1 one sees new advantages of the state-variable method[7] as well as added utility to gyrator replacements. The table design data for Table 1 is obtained by using the Holt–Taylor replacement[4] directly in Fig. 2.

Still other factors may be influential in a designer's choice of a given circuit, as, for example, the designer's familiarity with a given type of structure. Other more objective factors which seem to call for study and comparison at this point are: (1) bias circuitry and requirements, (2) obtainable Q ranges, (3) sensitivity to mask alignment and other integrated circuit processing, (4) noise behaviour.

Of course there are many other circuits which could be considered,[10, 11], and others which need further development,[12] but those discussed here

Table 1. *Total values of components*

Circuit	Total C	Total R (γ = gyrators)	C spread	R spread	Number of "active" elements
Table design	177·4 nf	r = 1·2 KΩ γ = 1·202 KΩ	26·4–62·3 nf	600 Ω	2 gyrators
Table replacement	241·4 pf	r = 1·2 KΩ γ = 695·2 KΩ	21·4–95·4 pf	600 Ω–316 KΩ	4 gyrators
Gyrator cascade	529 pf	r = 1·2 KΩ γ = 157·2 KΩ	32–302 pf	600 Ω–120 KΩ	5 gyrators
State variable	150 pf	56·16 KΩ	50 pf	30 Ω–15·2 KΩ	7 operational amplifiers
Lumped-distributed	1324 pf	228 KΩ	66–900 pf	10–178 KΩ	1 low gain
Low gain lumped	3761 pf	90 KΩ	358–1434 pf	10–40 KΩ	1 low gain
State-variable gyrator	750 pf	r = 93 KΩ γ = 594·4 KΩ	250 pf	56·5–118 KΩ	5 gyrators

give an excellent feeling for the optimal obtainable with complete integration. We mention, too, that the ungrounded-capacitor integrator has been emphasized in this paper, for Fig. 7, in contrast to the previously grounded one (Ref. (2), p. 70); this is due to the negative resistance introduced by the latter.[13] Although an improved grounded-capacitor integrator has been developed, its properties are still under investigation, while those of Fig. 5a are well known and assured workable.

"Where nothing else is seen, or heard, or known there is the Infinite."[1]

Acknowledgements—The support of the Air Force Office of Scientific Research under Contract AF-AFOSR F44620-67-C-0001 is gratefully acknowledged as is the interest of the students in the Stanford University course EE 367, Spring, 1969, and the checking of J. Miller. The joyful assistance of B. Conder in her very careful preparation of the text is truly appreciated with dedication too for her and for R. W. Lyman, a source of creative and educational progress.

REFERENCES

1. J. Mascaro (translator), *The Upanishads*. Penguin Books, Baltimore, 1965; from the *Chandogya Upanishad*, p. 119.
2. R. W. Newcomb, *Active Integrated Circuit Synthesis*. Prentice-Hall (1968).
3. J. K. Skwirzynski, *Design Theory and Data for Electrical Filters*. Van Nostrand (1965).
4. A. G. J. Holt and J. Taylor, Method of replacing ungrounded inductors by grounded gyrators. *Electron. Lett.* **1**, 105 (1965).
5. R. W. Newcomb, T. N. Rao and J. Woodard, A minimal capacitor cascade synthesis for integrated circuits. *Microelectron. & Reliab.* **6**, 113 (1967).
6. D. F. Sheahan, Gyrator-flotation circuit. *Electron. Lett.* **3**, 39 (1967).
7. W. J. Kerwin, L. P. Huelsman and R. W. Newcomb, State-variable synthesis for insensitive intecomb, State-variable synthesis for insensitive integrated circuit transfer functions. *IEEE Trans. Solid-St. Circuits* **SC-2**, 87 (1967).
8. W. J. Kerwin, Analysis and synthesis of active RC networks containing distributed and lumped elements. Stanford Electronics Laboratories, Technical Report No. 6560-14, August (1967).
9. P. Dewilde, L. Silverman and R. Newcomb, A passive synthesis for time-invariant transfer functions. *IEEE Trans. Circuit Theory*, accepted for publication.

10. L. P. HUELSMAN, *Theory and Design of Active RC Circuits*. McGraw-Hill (1968).

11. S. K. MITRA, *Analysis and Synthesis of Linear Active Networks*. John Wiley (1969).

12. E. B. KOZEMCHAK and R. W. NEWCOMB, State-variable synthesis of integrated-circuit distributed RC transfer functions. *Electron. Lett.* **4**, 320 (1968).

13. H. LANDSMAN, State-variable synthesis of active RC filters: a summary of theoretical techniques with physical constraints. *Papers on Integrated Circuit Synthesis*, III, compiled by R. W. NEWCOMB and M. B. WALDRON, Stanford Electronics Laboratories, Technical Report No. 6560-19, June (1969).